Towards open loop control of soft multistable grippers from energy-based modeling

Harith Morgan[1], Juan C. Osorio[1] and Andres F. Arrieta[1]

Abstract— Multistable structures are characterized by the existence of more than one statically stable state, which can provide a reference point for open-loop control schemes leveraging these systems' intrinsic mechanics. Multistable soft robots can thus take advantage of both the adaptability of soft robotics and the mechanical response of multistable elements for the potential simplification of robotic control and predictability. We present an energy-based analytical model for a class of soft multistable grippers enabling the design and prediction of their stable states abstracted as programmed operational points. The analytical model based on lumped parameter springs allows us to predict the system's final state upon actuation with reduced computational time compared to Finite Element (FE) simulations. The obtained computational efficiency enables us to search the configuration space in a tractable fashion, thereby facilitating the rational design of our grippers' set points. We validate our model against FE simulations and experimental tests. The model captures the fundamental mechanics of the introduced soft gripper topology, laying the foundation for efficient design optimization and simplified control of soft robots.

I. INTRODUCTION

Multistable soft robotic grippers are manipulators that leverage the adaptability of soft materials and the shape-shifting capabilities of multistable structures [1]. By utilizing the structure's mechanical response, the robot can achieve different global shapes which are predictable and energetically stable [2]. Compared with its rigid counterpart, incorporating soft materials into robots improves flexibility, adaptability, and compliance, highly increasing their degrees of freedom (DOF) [3], [4]. These key attributes offer soft robots several advantages over conventional hard robots, including facilitated human-machine interaction [5], [6], suitability for medical [7] and wearable devices [8], [9], and adaptability for gripping and manipulation [10]–[12].

Despite the recent progress, the infinite dimensionality, material non-linearity, and large deformations of most soft robots remain significant challenges that complicate their modeling and control [3], [5]. These factors result in the need for complex sensory systems and processing algorithms to implement closed-loop control [13]. One method for addressing this challenge is to take advantage of the energetically favorable configurations of multistable structures by utilizing its stable points to predict the final state of the robot just informed by the mechanics of the structure [2], [14].

Multistable structures are systems that display more than one energetically favorable configuration. They are often the result of a layering of multiple classical bistable substructures–including constrained beams/trusses[15], [16], constrained dielectric elastomers [17], shells [18], [19], compliant mechanisms [20], or balloon structures [21]. Applying multistable structures to soft robots can reduce the number of systems and complexity to achieve control in soft robotic devices [22]–[24], ultimately enhancing their functionality by providing the ability to reach desired set points without closed-loop feedback. As the robot reconfigures as it attains a new energy minimum, the adopted final state and shape can be predicted using its energy landscape (see Fig. 1b). However, the full potential of these devices can only be realized with the appropriate tools to overcome the challenges of targeted design, including modeling the complexities of interacting bistable units and long simulation run time when using conventional Finite Element (FE) packages [2], [25], [26].

This work introduces an energy-based analytical model that allows for shape prediction, targeted design, and control of a multistable soft robot gripper topology, the Dome Phalanx Gripper (DPG). Our topology enables the design of adaptable and robust grippers that exhibit desired stable states depending on the geometrical parameters of their constitutive bistable units. Our reduced order model incorporates lumped parameter spring elements that can capture the unit's bistable behavior, whose collective interactions dictate the soft robot's configuration and stiffness. This simplified model allows for input and shape parametrization, which can be utilized to predict the mechanics of any possible gripper geometric configuration. Our model ensures faster analysis time by leveraging a 2D lattice approximation [27] of the system and computing solutions through energy minimization processes, which can be utilized for faster design and accurate shape prediction for open-loop control.

II. MULTISTABLE STRUCTURES FOR OPEN LOOP CONTROL OF SOFT STRUCTURES

The DPG topology for which the model was based is composed of two equal pneumatic actuators with sequential bistable units (Fig. 1a (ii)). The actuator derives its multistable behavior from bistable domed-shaped shell elements (Fig. 1a (i)), and it can be geometrically tuned to reach and retain different final shapes after dome inversion (Fig. 1a (iii)). The designed stable states effectively discretized the infinite-dimensional deformation space into a tractable number of kinematic configurations, each attainable with open-loop inputs. The DPG performance and stable kinematic configurations can be tuned by changing the dome height (h), Unit Cell (UC) size, strain limiting thickness (t_L), air

[1]School of Mechanical Engineering, Purdue University, West Lafayette IN, USA aarrieta@purdue.edu

2023 IEEE International Conference on Soft Robotics (RoboSoft) | 979-8-3503-3222-3/23/$31.00 ©2023 IEEE | DOI: 10.1109/ROBOSOFT55895.2023.10121986

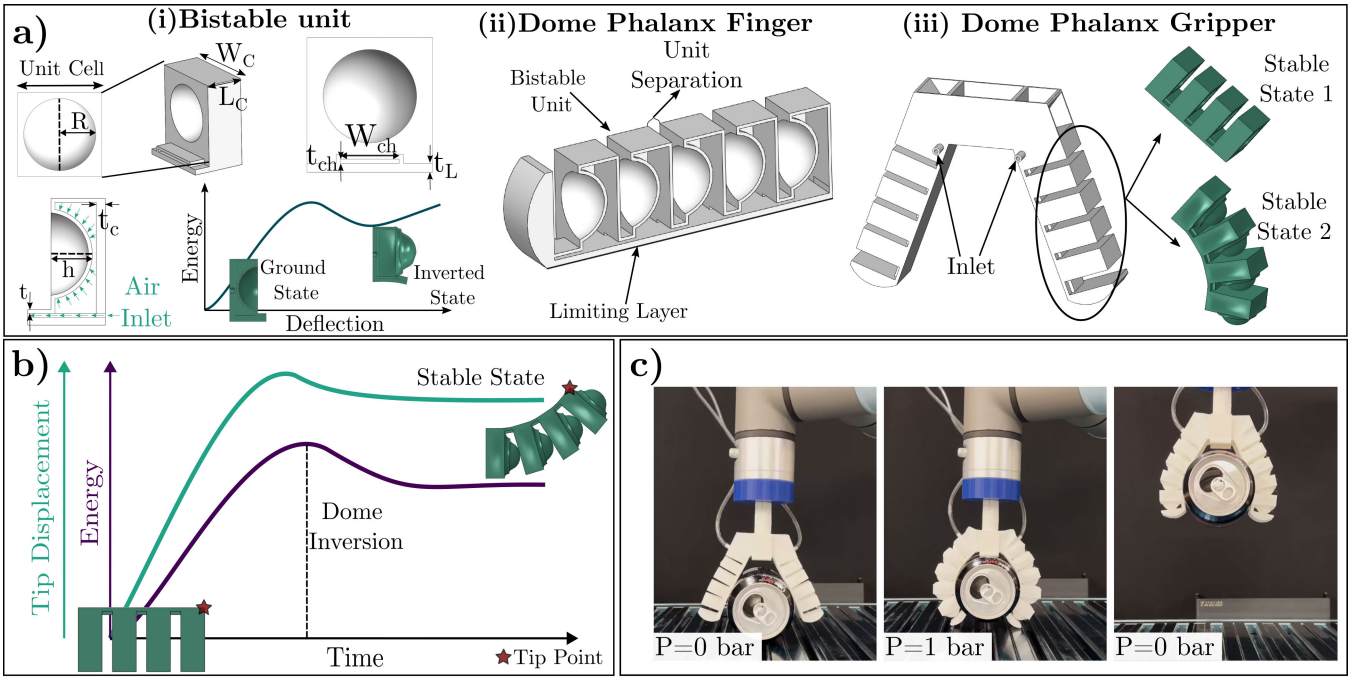

Fig. 1. Multistable soft gripper concept with embedded control from structural stability. a) (i) Bistable unit and its pneumatic actuation system. Dome unit geometric parameters: Unit cell (UC) size, h, t and R dome unit height, thickness, base radius, W_c, L_c and t_c chamber width length and thickness. W and t air_{ch} $channel_{ch}$ width and thickness, and t_L limiting layer thickness. (ii) Pneumatically actuated Dome Phalanx finger composed of bistable units with tunable unit separation. (iii) Dome Phalanx gripper (DPG) topology consisting of two soft fingers. Global stable states of the finger after bistable unit inversion. b) Schematic representation of the finger strain energy and tip displacement over time. The structure achieves a stable position and equilibrium after unit inversion without constant pressure actuation or retention. c) Experimental DPG behavior and carrying capacity (Movie 1).

chamber dimensions (W_c and L_c), and the spacing between adjacent cells (Unit Separation). Each of these features influences the interaction between neighboring segments, affecting the final state of the gripper, thus motivating the need for an efficient modeling framework. For these work, we selected the following parameters: h = 6.5 mm, t = 0.75 mm, R = 16 mm, UC = 22 mm, W_C = 20 mm, L_C = 9 mm, W_{ch} = 10 mm, t_{ch} = 0.75 mm, t_L = 1.5 mm, and Unit Separation of 3 mm. (see Fig. 1a for reference)

Bistable Unit: The system's bistable constitutive units are composed of a dome-shaped structure encapsulated by a square chamber that allows for pneumatic actuation and reset by applying positive and negative pressure, respectably (see Fig. 1a(i)). Each dome unit is geometrically bistable with two stable configurations [18], namely the stress-free and inverted states. Once the unit is fully inverted, contact between adjacent units and the strain-limiting layer induces the system's global curvature. The bistable domes on each finger segment support programmable deflections as the domes' final positions dictate the global kinematic configuration. The contact between the dome tip with the adjacent unit's chamber provides an additional interaction, contributing to the final curvature after all units are activated and the pressure is removed (see Movie 1 for details on gripper activation). The influences of bistable unit parameters are interrelated. The strain energy stored in the gripper topology in its activated states is the summation of the individual contributions from the inverted domes (see Fig. 1a). The magnitude of the interaction between neighboring domes is also affected by dome height (h) and chamber thickness (t_c). Together, dome height, and chamber thickness determine the degree of interaction between neighboring segments after dome inversion and yield the system's global curvature.

Control: The high-dimensionality and nonlinearity inherent to soft robots dramatically complicates closed-loop control schemes for such devices. Understanding the underlying mechanics governing the dome chamber characteristics and gripper's deflection provides the foundation for the rational design and simplified control of our DPGs. Developing the connection between input design parameters for the gripper and its kinematic response during activation creates the possibility of reliable open-loop control. To achieve this, a model to determine the DPG's kinematic configuration given a designed topology and a commanded input is needed. The multistability of our DPG gives the advantage programming multiple shape each associated with one energy minimum, as shown in fig. 1b. This allows structures to reach the desired position with minimal error and hold this position without constant actuation and closed-loop feedback.

III. ENERGY BASED MODEL FOR MULTISTABLE STRUCTURES

A. Model Derivation

Predicting the behavior of multistable DPGs requires consideration of both the unit cells' and the global geometric parameters. By characterizing the contribution of

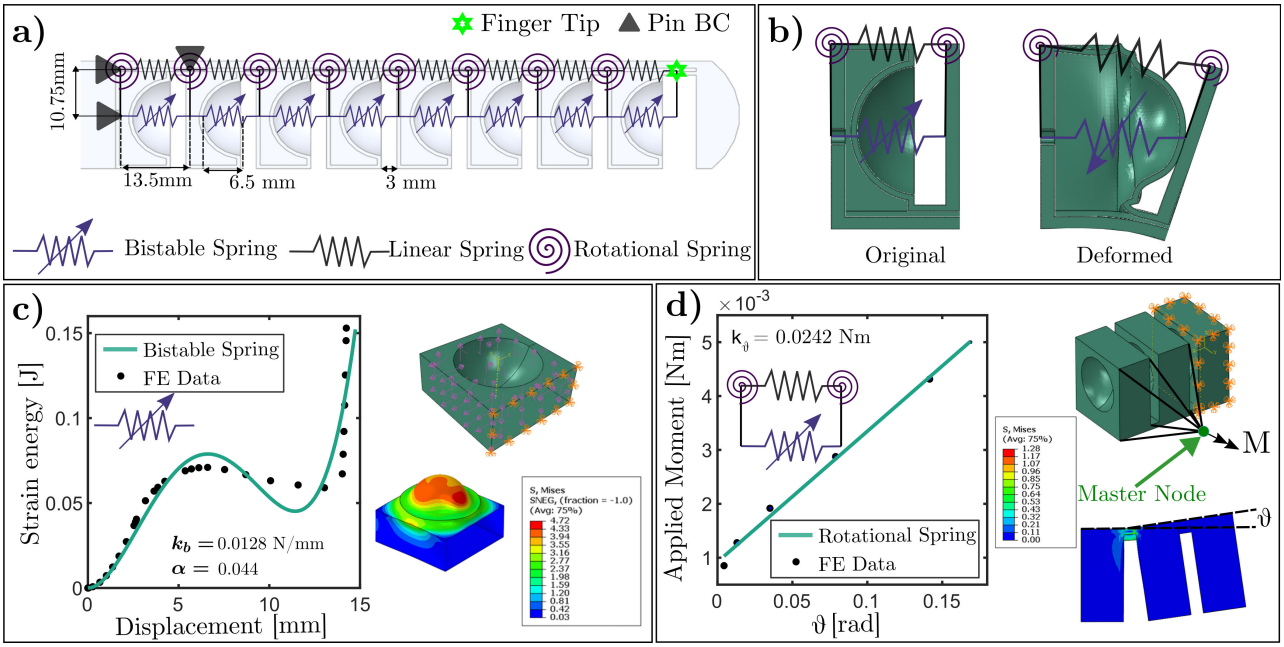

Fig. 2. Energy base model setup and parameter tuning. a) Spring lattice model for dome phalanx finger. b) Original and deformed configuration of bistable unit. c) Parameter tuning for bistable springs based on FE simulations. d) Parameter tuning for rotational springs based on FE simulations.

each DPGs subcomponents and their interactions, an energy landscape can be built where each minimum corresponds to a stable state of the system. The resulting strain from the energy minimization process dictates the programmed stable shapes with their geometrical and stiffness characteristics. We represent the DPG as a lattice comprising bistable, linear, and torsional springs (Fig. 2a). The springs' individual stiffness and connectivity allow us to map local extensions and rotations to defined energy contributions. We use bistable springs featuring a ground (unstressed) state and an inverted (stressed) to capture the influence of the bistable domes on the system. To appropriately represent the bistable dome behavior, we position the bistable springs so that the path of extension coincides with the dome's tip position between the ground and inverted states (see Fig. 2b).

The energy equation for the springs used in the lattice can be described as follows:

$$\text{Linear: } E_L = \frac{1}{2} k_l \cdot x^2$$

$$\text{Bistable: } E_{NL} = \frac{1}{2} k_b x^2 \left[1 + (1-\alpha) \left(\frac{x}{d} \right)^2 - 2 \frac{x}{d} \right]$$

$$\text{Torsional: } E_T = \frac{1}{2} k_\vartheta \cdot \vartheta^2$$

Linear springs capture connections between the bistable units, which are modeled as struts. In the DPG's case, the strain that these segments experience is negligible, behaving as a strain-limiting layer. Consequently, we model these connections as nearly rigid. While the axial strains experienced by this strain-limiting layer are negligible, the layer is sufficiently thick to display bending resistance. We capture the influence of this bending stiffness by introducing Torsional springs located at the nodes coincident with the strain-limiting layer. The angular displacement experienced by the torsional springs is dictated by the change in the angle ϑ formed by the segments (see Fig. 2d).

Minimizing the system's total energy, $E_{tot} = \sum_{i=1}^{n} E_L + E_{NL} + E_T$ where n is the number of units, constrains the space of possible interactions for the lattice elements into a discrete set of stable states. We employ the Newton-Raphson (NR) algorithm [28] to obtain the system's local minima as a function of the number of inverted units. The rich configuration space of our DPG requires establishing a rational method for providing the initial guess initializing the NR minimization process. To this end, we implement a geometric base model to generate initial guesses for the NR optimization so that the obtained states are in the neighborhood of physically feasible configurations with improved computational time.

B. Parameter Fitting

The lumped parameters capturing the linear, bistable, and torsional stiffnesses are fitted using a limited number of FE simulations of dome phalanx units. We tailor the model to our design topology by matching spring elements' lengths to the corresponding features of the gripper (Fig. 2a). By overlaying the lattice onto a cross-section of the dome phalanx gripper topology (Fig 2a), we can find a segment height and segment length of 10.75 mm and 13.5 mm, respectively. Our analysis allows us to obtain the constants within the spring energy formula: k_θ, k_b, and α, by simulating loads on the topology and measuring the appropriate deflections, reaction forces, and moments.

All FE simulations were performed using commercial software ABAQUS using 3D tetrahedral elements and dynamic implicit analysis to capture the systems' full actuation

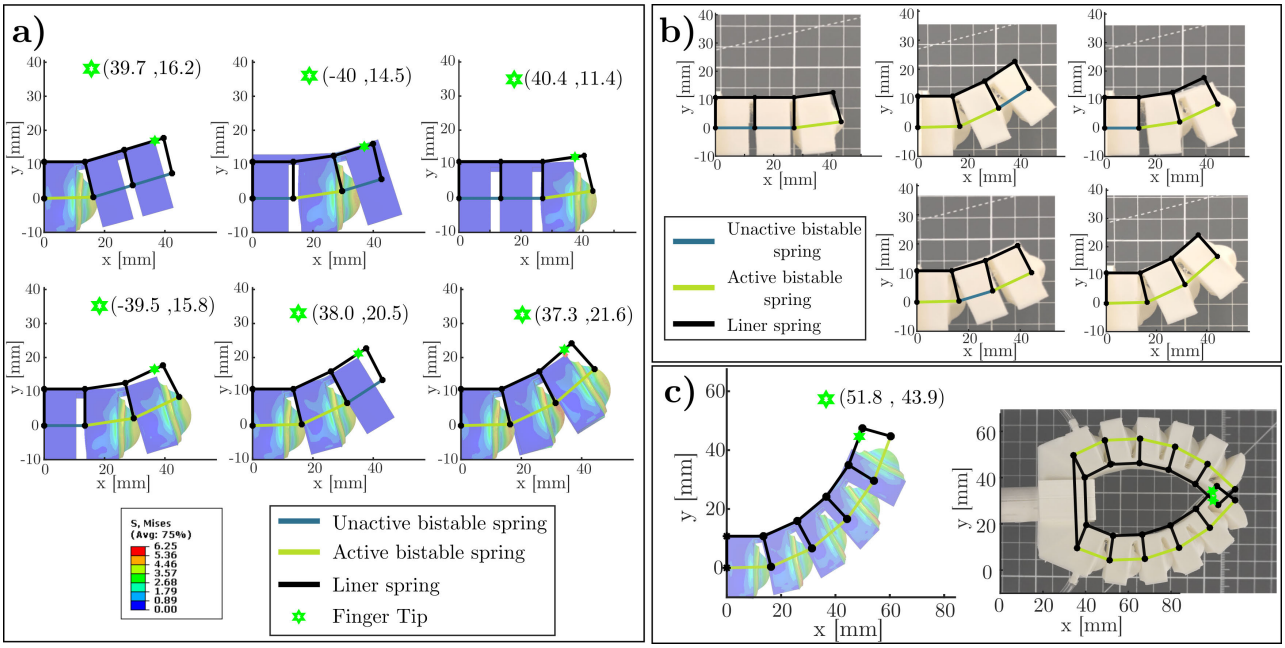

Fig. 3. Stable state prediction using energy base model and comparison with FE method simulations. a) 3-segment finger shape prediction with a different number of active bistable springs (Energy model vs FE Simulations). b) Experimental comparison for a 3-segment finger shape prediction using energy based model. c) Prediction for five-segment finger and extension for soft gripper topology.

path. A quasi-static dynamic implicit analysis with nonlinear behavior is used to capture the snap-through instability as each dome transitions from the ground to the inverted state. Every dome is actuated to the inverted state by applying constant pressure to each unit, and stability is guaranteed by adding relaxing steps after inversion. We used a linear elastic material model with modulus E = 26 MPa, corresponding to Ultimaker thermoplastic polyurethane (TPU) 95A [29].

Bistable Springs: First, we consider the extension length between bistable states (d). This parameter depends on the dome height for a given segment and can be interpreted as the extension length between stable states. For this particular case, we can use a value of d = 3.5 mm, corresponding to dome height h minus the unit separation. The remaining parameters of the bistable energy formula, k_b and α, are determined via FE Analysis and curve fitting (Fig. 2c). We apply a ramping pressure load from 0 to 0.15 MPa on the interior surfaces of the dome chamber. During the process of inversion, the strain energy of the system increases to reflect the energy stored in the bistable structure. The displacement of the dome's tip corresponds to the extension length of the model's bistable spring. Correspondingly, the resulting strain energy captures the behavior of the bistable spring. By performing this analysis and utilizing the least squares curve fitting technique, we calculate the stiffness k_b as 12.84 N/mm, and the non-dimensional force linearity constant α is 0.043.

Torsional Springs: To determine the torsional stiffness, k_θ, we simulate an applied moment of maximum amplitude 0.005 Nm to the latter two segments of DPG comprised of three dome phalanxes (see Fig. 2d). The moment is applied using tied elements that numerically bind a reference point (master node) to the two dome phalanx segments, as shown in Fig. 2d. We track the movement of the limiting layer and calculate the roataion angel ϑ. A linear correlation between the rotation angle and the applied moment is observed, which confirms linear behavior of our torsional spring with a best fit slope of k_ϑ = 0.0242 Nm/rad.

C. Stable states prediction and performance

Using the parameters from the fitting process, we are able to predict stable state configurations for the DPG with the resulting model. Given that the bistable elements of the gripper are independently stable, the expected number of states for a given dome phalanx finger topology follows 2^n, where n is the number of segments on the finger. We use this knowledge, coupled with our ability to design for desired configurations to cycle through all 2^n possibilities to reveal the complete map of stable states for a given topology (Fig. 3a). This means that we can quickly generate maps yielding the positioning and grasp configuration for any given design implementation of the DPG as a function of the number of bistable units, h, unit separation, and UC size. This parametric design space search is enabled by the tractability of our model, allowing us to efficiently assess different design implementations of the DPG (Fig. 1c) and determine suitability for the desired task. One example is A DPG designed to handle aluminum cans (see Movie 1).

The model can determine the behavior of a given gripper design in orders of magnitude less time than the FE numerical simulations, which makes it feasible for iterating through potential configurations and optimizing for the best design according to a given task (e.g., position and grasping force).

FE model validation: We validate our spring lattice

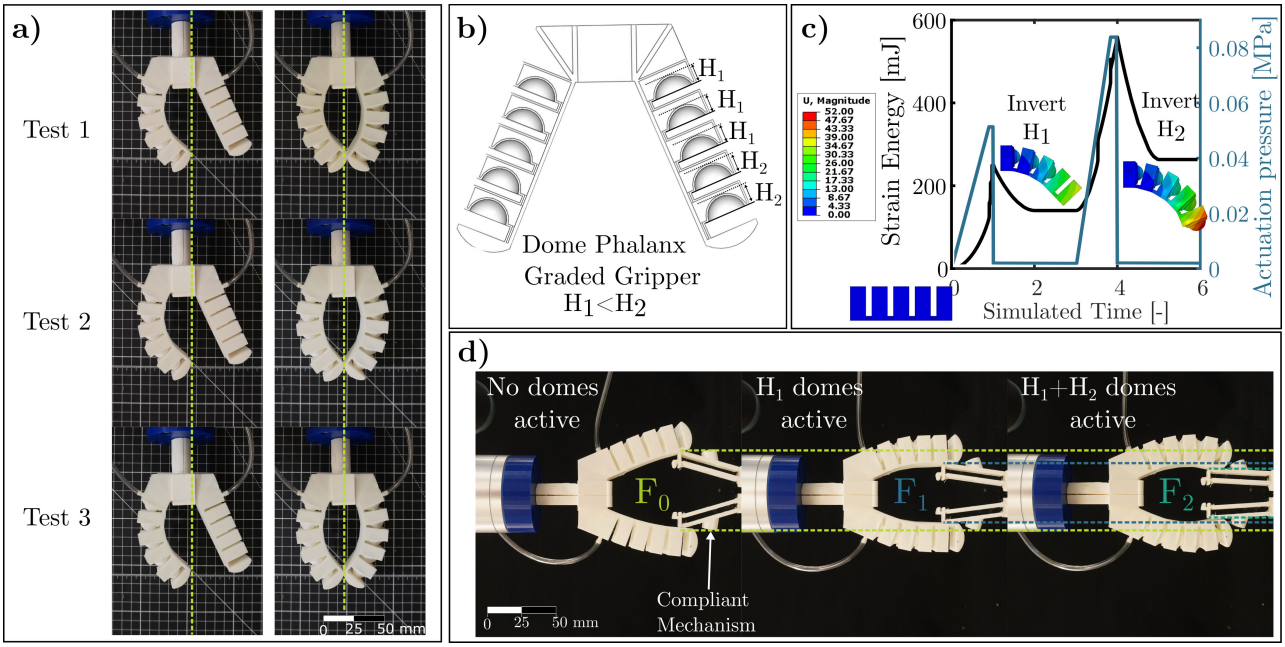

Fig. 4. Dome phalanx gripper performance tests. a) Soft gripper position control tests. The gripper achieves a stable position that can be predicted with the energy base model. b) Graded dome height gripper geometry ($H_1 < H_2$) allows accessible, stable states using different pressure inputs. c) Different energy minima and stable states of the graded dome height finger, $H_1 = 6.5$ mm and $H_2 = 7.5$ mm (FE analysis). d) Force control tests. Different numbers of inverted domes lead to distinct grasping forces ($F_0 < F_1 < F_2$). Force increase is represented by further compression of the compliant mechanism.

model against FE simulations and experimental tests (Fig. 3a and Fig. 3b). Given our fitting process, FE simulations are our direct basis of comparison–where we closely calculate associated run time and errors–whereas we use experimental results as a qualitative validation of the overall predictive capacity of the model. Calculating the stable configurations of a three-segment DPG sample (Fig 3a) via FE simulation required between 20 and 80 min, whereas, the same calculations via the spring lattice model required fewer than 30 seconds. That is a time reduction by more than $\frac{1}{200}$. With such a significant reduction in computation time, the spring lattice model maintained prediction errors below 15% for the three segment dome phalanx finger stable state calculations. We repeat this same comparison with a five segmented DPG (Fig 3c), where the model was able to determine the position and tip deflection of a fully activated gripper in 0.85 minutes. In this case the model was able to reduce the computation time by more than $\frac{1}{300}$ whilst accruing only a 12% error.

Experimental Validation: We further illustrate the viability of the energy-based spring lattice model as a design tool by comparing model predictions against experimental results. We used the exact design implementation shown in Fig 3a and 3D printed a DPG sample using TPU. Each sample was printed using the FDM printing technique on an Ultimaker 3d printer. Layer height was reduced to avoid air leakages and guarantee pneumatic actuation of the DPG. We compared the different actuated configurations of the DPG sample with an overlay of the corresponding model prediction. Notably, we can predict both the DPG sample tip deflection and overall kinematic configuration (see Fig. 3b).

IV. SOFT GRIPPER DESIGN AND PERFORMANCE

The model's efficacy is further illustrated by predicting the grasp curvature and aperture for a complete DPG (see Fig. 3c). We leverage the model capacity by joining two phalanx fingers as a gripper and predicting the system's resulting shape, showing full closure after all units are inverted. It should be noted that contact is not included in the model resulting in overlap between each finger's predicted shapes.

Position Control: To illustrate the model's capability as a design tool, we tested the ability of several specimens to achieve reliably desired shapes. The topologies generated by the model show deterministic behavior, meaning the achieved kinematical states are attained as long as the gripper geometric parameters remain unchanged (see Fig 4a and Movie 1). Specifically, we cycle each gripper's digit between the base and fully activated states, verifying the gripper's ability to attain the same aperture and positioning across cycles. This characteristic allows for robust robot design, as the bistable elements provide intrinsic kinematic control dictated by the gripper's mechanical response. The position control inherent to the designed multistable structure can serve as set points for triggering different control actions.

Force Control: We further leverage the characteristics of our multistable DPG by locally modifying the dome height resulting in a geometric grading that generates more accessible stable states by modulating the pneumatic actuation pressure (see Figs. 4b and 4c). The additionally accessible minima to the system can be utilized to achieve control of the DPG's final shape and grasping force. To illustrate this, we 3D printed a gripper topology with two distinct dome heights (H_1 and H_2 see Fig. 4b). As $H_1 < H_2$, the first three

units (H_1) invert at a lower pressure value than the last two (H_2). This allows for controlling the grasping position and force of the system simply by modulating the input pressure. To test this, we utilized compliant mechanisms composed of two bars that compress once the grasping force increases. We characterized the mechanism's force vs. aperture to measure the gripper's grasping force (see Movie 1). Our experiments show that the selective inversion of domes results in different force magnitudes (F_0, F_1, and F_2) while reducing the aperture of the mechanism. For this particular geometry, we measure a maximum force F_2 = 1.28 N when all domes are activated and an intermediate force of F_1 = 0.91 N when H_1 domes are inverted. Therefore, we can achieve open-loop modulation of the DPG's grasping force as a function of the number of inverted units increasing it up to 2X force factor. Consequently, by controlling the number of inverted units, we can control the tip position and grasping force of our DPG without sensors or closed-loop control.

V. CONCLUSIONS AND FUTURE WORK

We present an energy-based method for modeling the mechanics of Dome Phalanx Grippers leveraging a novel multistable architecture for soft grippers. The derived lumped parameter model and parameter fitting procedure allowed for capturing the multiple kinematic configurations of FE and experimental specimens with errors below 15 %. We used the design capacity of our model to design DPG with many accessible states. Notably, we show that we can modulate the DPG gripping force to a known value without closed-loop control. The results support the viability of our energy-based spring lattice model as a tool for elucidating the behavior of soft robotic gripper topologies and, ultimately, for facilitating open-loop control of soft robotic grippers. Furthermore, this suggests a path toward the targeted design of robust multistable soft robotic grippers with control embedded in the mechanical response of the system. Future work will focus on establishing forward design tools that yield DPG topologies directly from desired properties and producing tailored grasping routines without feedback control.

ACKNOWLEDGMENTS

We acknowledge the support of the NSF-CAREER award No. 1944597. H.M. thanks the support the Knox fellowship from Purdue University's Graduate School.

REFERENCES

[1] A. Pal, V. Restrepo, D. Goswami, and R. V. Martinez, "Exploiting mechanical instabilities in soft robotics: Control, sensing, and actuation," Advanced Materials, vol. 33, p. 2006939, 5 2021.

[2] J. C. Osorio, H. Morgan, and A. F. Arrieta, "Programmable multistable soft grippers," in 2022 IEEE 5th International Conference on Soft Robotics (RoboSoft), 2022, pp. 525–530.

[3] G. M. Whitesides, "Soft robotics," Angewandte Chemie - International Edition, vol. 57, 2018.

[4] D. Rus and M. T. Tolley, "Design, fabrication and control of soft robots," Nature, vol. 521, pp. 467–475, 5 2015.

[5] C. Lee, M. Kim, Y. J. Kim, N. Hong, S. Ryu, H. J. Kim, and S. Kim, "Soft robot review," International Journal of Control, Automation and Systems, vol. 15, 2017.

[6] C. Majidi, "Soft robotics: A perspective - current trends and prospects for the future," Soft Robotics, vol. 1, 2014.

[7] T. Deng, H. Wang, W. Chen, X. Wang, and R. Pfeifer, "Development of a new cable-driven soft robot for cardiac ablation," in 2013 IEEE International Conference on Robotics and Biomimetics, ROBIO 2013, 2013.

[8] P. Polygerinos, Z. Wang, K. C. Galloway, R. J. Wood, and C. J. Walsh, "Soft robotic glove for combined assistance and at-home rehabilitation," in Robotics and Autonomous Systems, vol. 73, 2015.

[9] A. T. Asbeck, S. M. D. Rossi, K. G. Holt, and C. J. Walsh, "A biologically inspired soft exosuit for walking assistance," International Journal of Robotics Research, vol. 34, 2015.

[10] C. Santina, R. K. Katzschmann, A. Bicchi, and D. Rus, "Model-based dynamic feedback control of a planar soft robot: trajectory tracking and interaction with the environment," International Journal of Robotics Research, vol. 39, 2020.

[11] M. Calisti, M. Giorelli, G. Levy, B. Mazzolai, B. Hochner, C. Laschi, and P. Dario, "An octopus-bioinspired solution to movement and manipulation for soft robots," Bioinspiration and Biomimetics, vol. 6, 2011.

[12] R. K. Katzschmann, A. D. Marchese, and D. Rus, "Autonomous object manipulation using a soft planar grasping manipulator," Soft Robotics, vol. 2, 2015.

[13] T. G. Thuruthel, B. Shih, C. Laschi, and M. T. Tolley, "Soft robot perception using embedded soft sensors and recurrent neural networks," Science Robotics, vol. 4, no. 26, 2019.

[14] D. Melancon, A. E. Forte, L. M. Kamp, B. Gorissen, and K. Bertoldi, "Inflatable origami: Multimodal deformation via multistability," Advanced Functional Materials, 2022.

[15] D. Restrepo, N. D. Mankame, and P. D. Zavattieri, "Phase transforming cellular materials," Extreme Mechanics Letters, vol. 4, pp. 52–60, 9 2015.

[16] D. M. Boston, F. R. Phillips, T. C. Henry, and A. F. Arrieta, "Spanwise wing morphing using multistable cellular metastructures," Extreme Mechanics Letters, vol. 53, p. 101706, 5 2022.

[17] J. Zhao, S. Wang, D. McCoul, Z. Xing, B. Huang, L. Liu, and J. Leng, "Bistable dielectric elastomer minimum energy structures," Smart Materials and Structures, vol. 25, 6 2016.

[18] J. A. Faber, J. P. Udani, K. S. Riley, A. R. Studart, and A. F. Arrieta, "Dome-patterned metamaterial sheets," Advanced Science, vol. 7, no. 22, p. 2001955, 2020.

[19] J. P. Udani and A. F. Arrieta, "Taming geometric frustration by leveraging structural elasticity," Materials & Design, vol. 221, p. 110809, 9 2022.

[20] Y. S. Oh and S. Kota, "Synthesis of Multistable Equilibrium Compliant Mechanisms Using Combinations of Bistable Mechanisms," Journal of Mechanical Design, vol. 131, no. 2, 01 2009, 021002.

[21] Y. Chi, Y. Li, Y. Zhao, Y. Hong, Y. Tang, and J. Yin, "Bistable and multistable actuators for soft robots: Structures, materials, and functionalities," Advanced Materials, vol. 34, 2022.

[22] G. Kofod, M. Paajanen, and S. Bauer, "Self-organized minimum-energy structures for dielectric elastomer actuators," Applied Physics A: Materials Science and Processing, vol. 85, no. 2, pp. 141–143, 2006.

[23] M. T. Petralia and R. J. Wood, "Fabrication and analysis of dielectric-elastomer minimum-energy structures for highly-deformable soft robotic systems," IEEE/RSJ 2010 International Conference on Intelligent Robots and Systems, IROS 2010 - Conference Proceedings, pp. 2357–2363, 2010.

[24] L. C. van Laake, J. de Vries, S. M. Kani, and J. T. Overvelde, "A fluidic relaxation oscillator for reprogrammable sequential actuation in soft robots," Matter, vol. 5, pp. 2898–2917, 9 2022.

[25] G. Gerboni, A. Diodato, G. Ciuti, M. Cianchetti, and A. Menciassi, "Feedback control of soft robot actuators via commercial flex bend sensors," IEEE/ASME Transactions on Mechatronics, vol. 22, no. 4, pp. 1881–1888, 2017.

[26] J. M. Bern, Y. Schnider, P. Banzet, N. Kumar, and S. Coros, "Soft robot control with a learned differentiable model," in 2020 3rd IEEE International Conference on Soft Robotics (RoboSoft), 2020, pp. 417–423.

[27] J. Meaud, "Multistable two-dimensional spring-mass lattices with tunable band gaps and wave directionality," Journal of Sound and Vibration, vol. 434, 2018.

[28] C. T. Kelley, "Solving nonlinear equations with newton's method," Solving Nonlinear Equations with Newton's Method, 1 2003.

[29] Ultimaker, "Technical data sheet TPU 95A," pp. 1–3, 2017.